Global Ultrasound Elastography in Spatial and Temporal Domains

Md Ashikuzzaman, Claudine J. Gauthier and Hassan Rivaz

This supplementary material contains an analysis on how regularization parameters depend on ultrasound frame rate (Fig. 1). In addition, we present a comprehensive comparison of Hybrid, GLUE and GUEST methods for different strain levels (Fig. 2). We also include a simulation experiment with temporally irregular frames to show the robustness of our method to varying velocity of the probe during free-hand palpation (Fig. 3). Additionally, we present a simulation experiment with a phantom containing an inclusion with intra-varying elasticities (Fig. 4 and Table I). Axial strain images from GUEST for a simulation phantom with different sets of parameter values have been reported (Fig. 5). Finally, we show the strain profiles obtained from Hybrid, GLUE and GUEST over a vertical cut of the simulation data (Fig. 6).

I. Results

Fig. 1 presents the strain images from GUEST for a simulation phantom with frame to frame strains 0.5% and 3%. For both simulations, regularization parameters were kept the same (α_1=5, α_2=1, α_3=20, β_1=5, β_2=1 and β_3=20). Optimal results for both cases were obtained using the aforesaid parameter settings. This proves that parameter values do not depend on strain percentage which in turn says that parameter values are unrelated to the rate of ultrasound data acquisition.

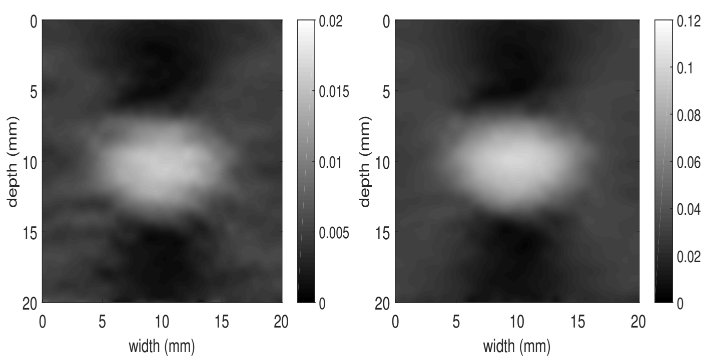

Fig. 1: Axial strain images from GUEST for the simulation phantom with different strain level. First and second columns correspond to the axial strain images for frame to frame strains of 0.5% and 3% respectively.

Fig. 2 shows the strain images and histograms of CNR values for a simulation phantom with frame to frame strain of 1%, 2% and 3%. In Fig. 2(c), sliding blue target and red background windows for calculating 120 (6 target and 20 background windows) CNR values are shown. Histograms with 120 CNR values are also presented in Fig. 2. Both visual assessment and histograms suggest that GUEST produces better strain images than GLUE and the Hybrid method.

We have simulated a situation where Radio-Frequency (RF) frames are temporally irregular. The strain from first frame to second frame is 0.5% and second frame to third frame is 0.6%. Fig. 3 depicts that GUEST is successful in obtaining a correct strain map even for this temporally discontinuous case. This experiment supports our claim that GUEST is robust to temporal irregularity induced from sinusoidal hand motion or other sources.

We have simulated a homogeneous phantom with an elasticity of 20 kPa using Field II. The simulated phantom contains a hard inclusion with intra-varying elasticity levels of 40 kPa and 80 kPa. We have compressed the phantom using closed form equations. Let us consider the axial and lateral positions of a particular scatterer are z_p and x_p. Lateral displacement of the scatterer is given by:

$$d_x(x_p) = \begin{cases} \nu s_1 x_p & \text{if } z_p \leq D_1 \\ \nu s_2 x_p & \text{if } D_1 < z_p \leq D_2 \\ \nu s_3 x_p & \text{if } D_2 < z_p \leq D_3 \\ \nu s_1 x_p & \text{otherwise} \end{cases} \tag{1}$$

Here, ν is poisson's ratio which is considered to be 0.49 for this experiment. s_1 stands for the percent axial strain in background. s_2 and s_3 are percent strains in the portions of the hard inclusion with elasticities 40 kPa and 80 kPa respectively. $D_1 < z_p \leq D_2$ corresponds to the axial positions with an elasticity of 40 kPa. Similarly, $D_2 < z_p \leq D_3$ is the depth of the tissue with an elasticity of 80 kPa. Axial shift of the scatterer is given by Eq. 2.

$$d_z(z_p) = \begin{cases} -s_1 z_p & \text{if } z_p \leq D_1 \\ -s_2(z_p - D_1) - s_1 D_1 & \text{if } D_1 < z_p \leq D_2 \\ -s_3(z_p - D_2) - s_2(D_2 - D_1) - s_1 D_1 & \text{if } D_2 < z_p \leq D_3 \\ -s_1(z_p - D_3) - s_3(D_3 - D_2) - s_2(D_2 - D_1) - s_1 D_1 & \text{otherwise} \end{cases} \tag{2}$$

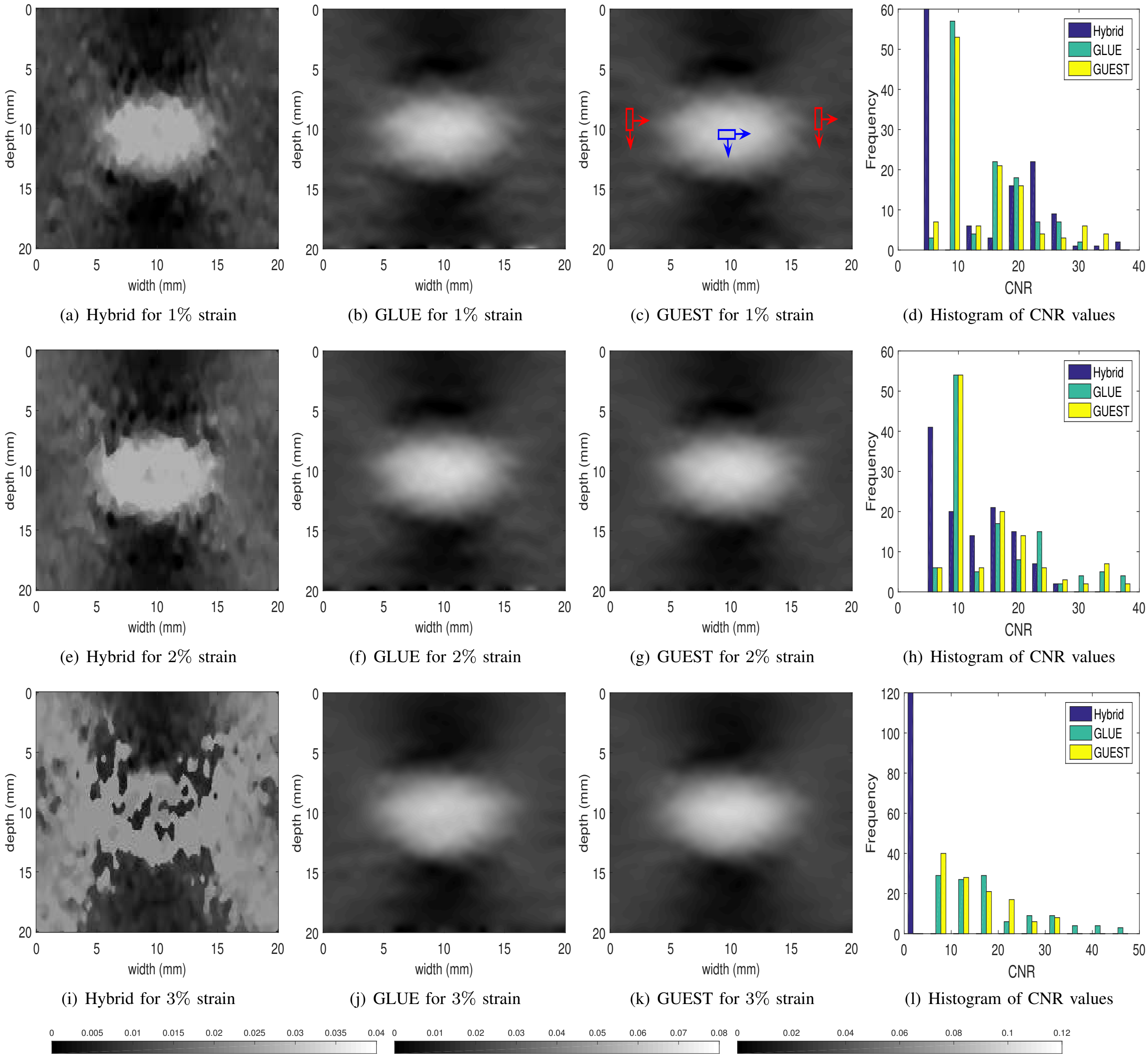

(a) Hybrid for 1% strain (b) GLUE for 1% strain (c) GUEST for 1% strain (d) Histogram of CNR values

(e) Hybrid for 2% strain (f) GLUE for 2% strain (g) GUEST for 2% strain (h) Histogram of CNR values

(i) Hybrid for 3% strain (j) GLUE for 3% strain (k) GUEST for 3% strain (l) Histogram of CNR values

(m) Color bar for 1% strain (n) Color bar for 2% strain (o) Color bar for 3% strain

Fig. 2: Axial strain images and histograms for the simulation phantom. Rows 1, 2 and 3 correspond to frame to frame strain levels of 1%, 2% and 3% respectively. Columns 1-3 show strain images for Hybrid, GLUE and GUEST respectively. Column 4 presents the histograms of CNR values. (m), (n) and (o) correspond to color bars for 1%, 2% and 3% strains respectively.

In this experiment, s_1 is considered to be 4%. To comment on s_2 and s_3, let's revisit two basic physics concepts. First, Hooke's law: $\sigma = sE$. Here, σ, s and E correspond to stress, strain and elasticity of a portion of the tissue. Second, equilibrium which means that stresses in different portions of the tissue are equal. In light of these two basic rules, s_2 and s_3 turn out to be 2% and 1% respectively. The ideal and estimated axial strain images from Hybrid, GLUE and GUEST for the simulated phantom are presented in Fig. 4. It is visually clear that the strain image from GUEST shows the boundaries of different layers better than Hybrid and GLUE. Quantitative values of Peak-Signal-to-Noise Ratio (PSNR) and Structural Similarity Index (SSIM) are reported in Table I. GUEST provides the highest values for both of the metrics. This particular experiment proves that our method does not over-smooth the strain image. Instead, GUEST better depicts different layers of the tissue than the existing methods.

In Fig. 5, we have presented axial strain images from GUEST for simulation phantom with different sets of parameter values. We have reported results for $\alpha_1 = \beta_1 = 0, 1, 2, 5$.

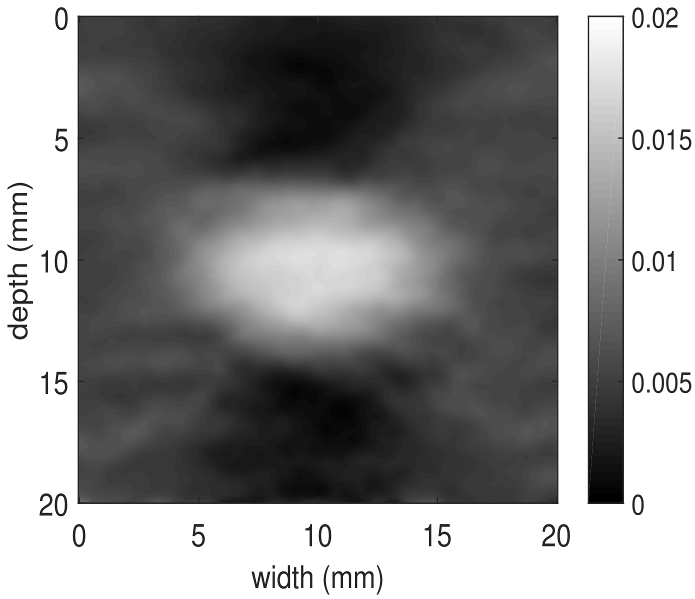

Fig. 3: Axial strain image from GUEST for the simulation phantom with temporal discontinuity.

TABLE I: SSIM and PSNR of the strain images for simulation phantom with an inclusion with intra-variation in elasticity.

	SSIM	PSNR (dB)
Hybrid	0.7280	45.7951
GLUE	0.9479	46.6852
GUEST	**0.9509**	**46.8747**

For all four cases of α_1 and β_1, α_2 and β_2 are kept constant at 1 while α_3 and β_3 are set to 20. Additionally, we report results for $\alpha_2 = \beta_2 = 0, 0.1, 0.5, 1$ setting α_1, β_1, α_3 and β_3 to $5, 5, 20$ and 20 respectively. Finally, we have presented axial strain images for $\alpha_3 = \beta_3 = 0, 1, 5, 20$ while α_1, β_1, α_2 and β_2 remain fixed at $5, 5, 1$ and 1 respectively. This experiment shows the dependence of strain estimation on different regularization parameters. Fig. 6 shows the strain profiles from Hybrid, GLUE and GUEST for the simulation data over a vertical cut. GUEST generates a smoother strain profile in uniform regions compared to both GLUE and the Hybrid methods. The strain plot from Hybrid suffers from a large fluctuation of background strain. The diameter of the inclusion is marked with ticks in the x-axis of the strain profile figure.

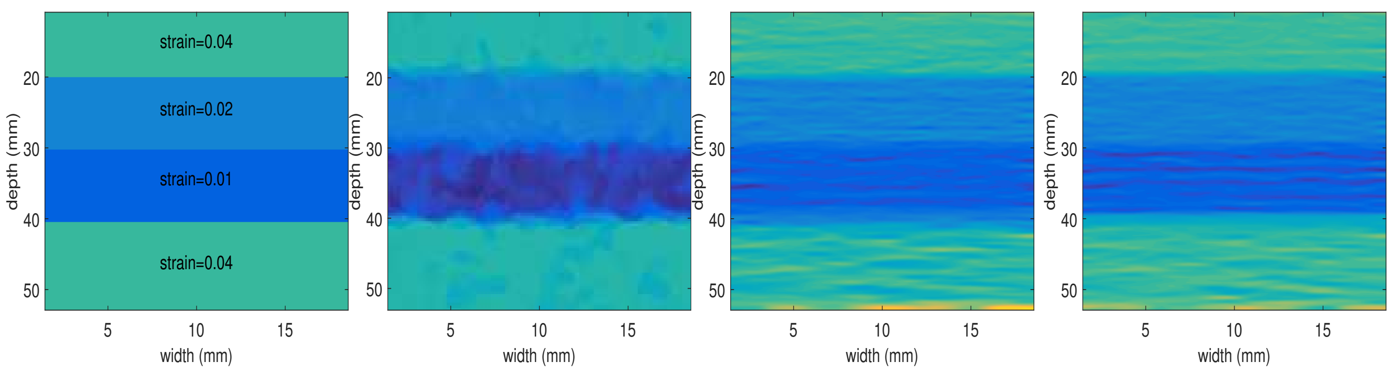

(a) Ideal strain (b) Hybrid (c) GLUE (d) GUEST

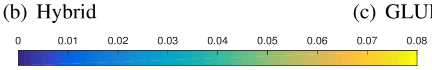

(e) Color bar

Fig. 4: Axial strain images for a simulation phantom with an inclusion containing intra-variation in elasticity. Column 1 represents the ideal strain image. Columns 2-4 show strain images for Hybrid, GLUE and GUEST respectively. (e) represents the color bar.

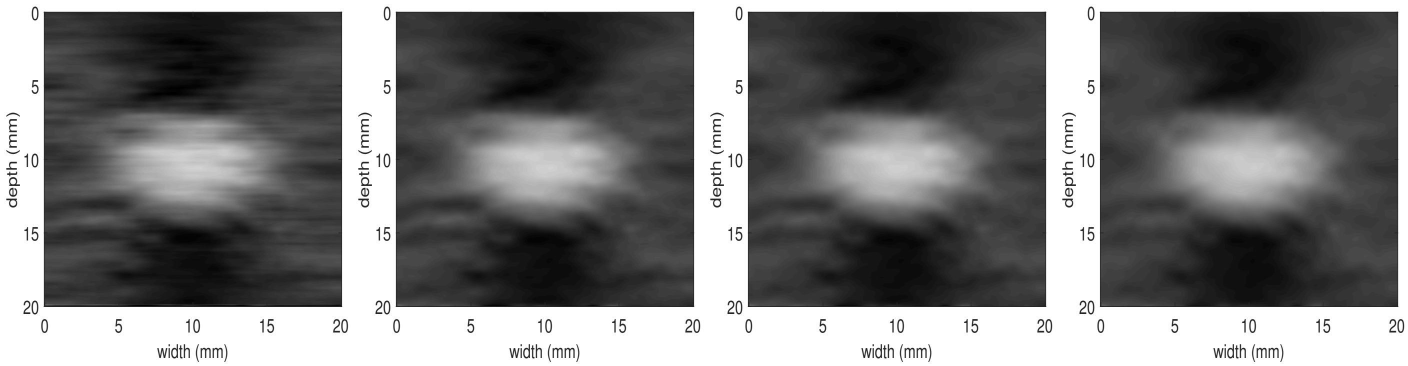

(a) $\alpha_1 = \beta_1 = 0$, $\alpha_2 = \beta_2 = 1$, $\alpha_3 = \beta_3 = 20$ (b) $\alpha_1 = \beta_1 = 1$, $\alpha_2 = \beta_2 = 1$, $\alpha_3 = \beta_3 = 20$ (c) $\alpha_1 = \beta_1 = 2$, $\alpha_2 = \beta_2 = 1$, $\alpha_3 = \beta_3 = 20$ (d) $\alpha_1 = \beta_1 = 5$, $\alpha_2 = \beta_2 = 1$, $\alpha_3 = \beta_3 = 20$

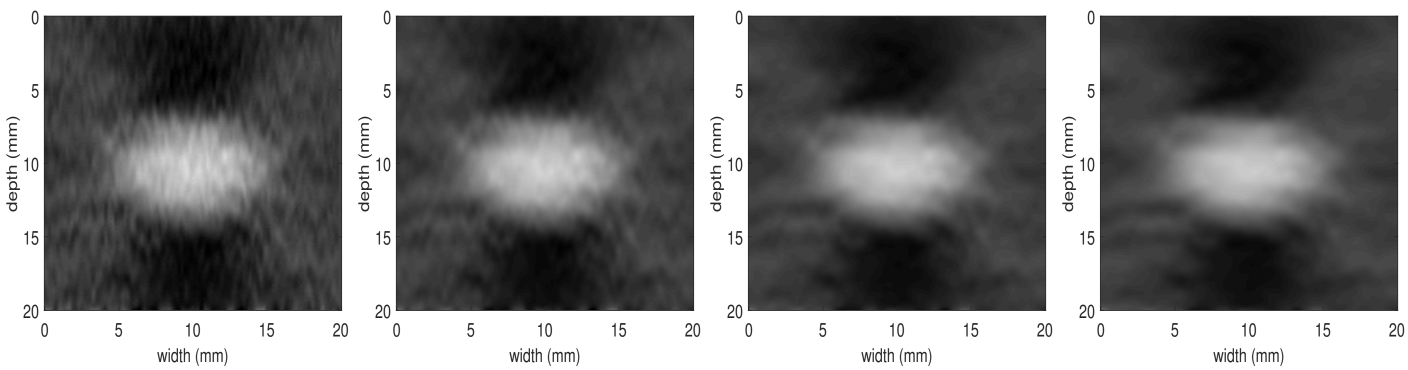

(e) $\alpha_1 = \beta_1 = 5$, $\alpha_2 = \beta_2 = 0$, $\alpha_3 = \beta_3 = 20$ (f) $\alpha_1 = \beta_1 = 5$, $\alpha_2 = \beta_2 = 0.1$, $\alpha_3 = \beta_3 = 20$ (g) $\alpha_1 = \beta_1 = 5$, $\alpha_2 = \beta_2 = 0.5$, $\alpha_3 = \beta_3 = 20$ (h) $\alpha_1 = \beta_1 = 5$, $\alpha_2 = \beta_2 = 1$, $\alpha_3 = \beta_3 = 20$

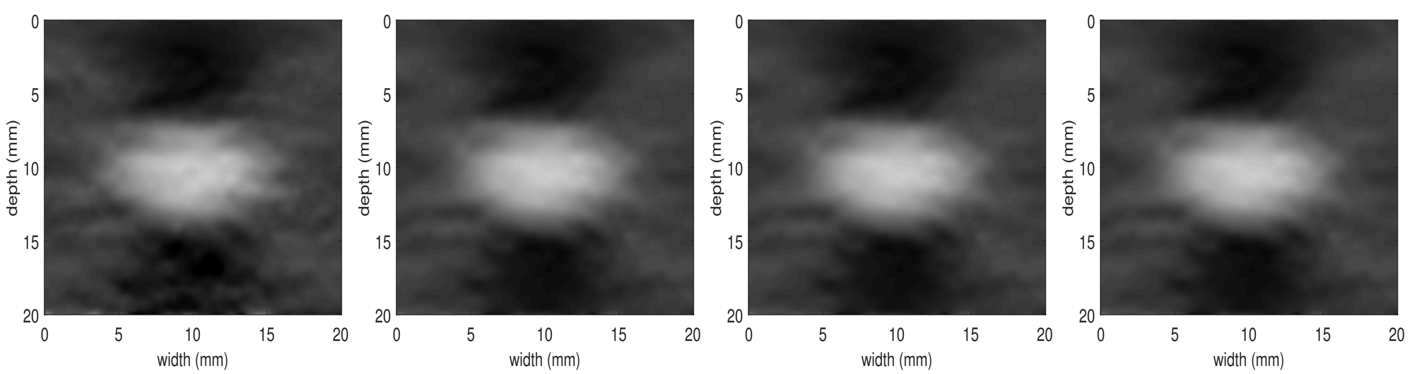

(i) $\alpha_1 = \beta_1 = 5$, $\alpha_2 = \beta_2 = 1$, $\alpha_3 = \beta_3 = 0$ (j) $\alpha_1 = \beta_1 = 5$, $\alpha_2 = \beta_2 = 1$, $\alpha_3 = \beta_3 = 1$ (k) $\alpha_1 = \beta_1 = 5$, $\alpha_2 = \beta_2 = 1$, $\alpha_3 = \beta_3 = 5$ (l) $\alpha_1 = \beta_1 = 5$, $\alpha_2 = \beta_2 = 1$, $\alpha_3 = \beta_3 = 20$

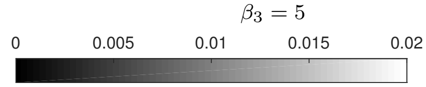

(m) Color bar

Fig. 5: Axial strain images for simulation phantom with different sets of regularization parameter values. Rows 1 shows the axial strain images for different values of α_1 and β_1. Rows 2 represents changes in axial strain images by varying α_2 and β_2. Rows 3 corresponds to the axial strain images for different values of α_3 and β_3. (m) represents the color bar.

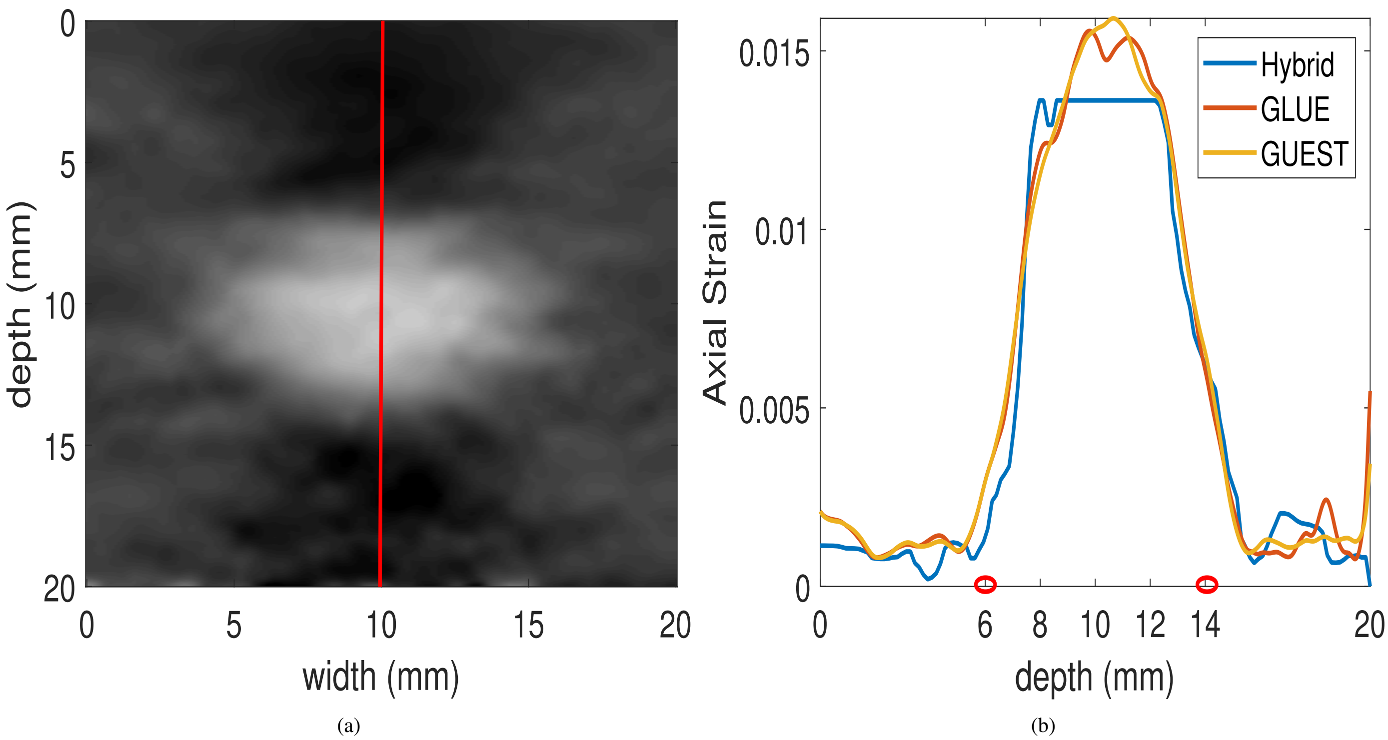

Fig. 6: One dimensional strain profile. (a) shows the vertical line whose strain is plotted. (b) represents the strain profiles obtained from Hybrid, GLUE and GUEST. Red marked ticks on the horizontal axis represent the beginning and end of the inclusion.